

# Diffusion Tensor Imaging to Predict Long-term Outcome after Cardiac Arrest

## A Bicentric Pilot Study

Charles-Edouard Luyt, M.D., Ph.D.,\* Damien Galanaud, M.D., Ph.D.,† Vincent Perlbarg, Ph.D.,‡ Audrey Vanhauzenhuysse, Ph.D.,§ Robert D. Stevens, M.D.,|| Rajiv Gupta, M.D.,# Hortense Besancenot, M.D.,\*\* Alexandre Krainik, M.D.,†† Gérard Audibert, M.D.,‡‡ Alain Combes, M.D., Ph.D.,§§ Jean Chastre, M.D.,§§ Habib Benali, Ph.D.,|||| Steven Laureys, M.D., Ph.D.,§ Louis Puybasset, M.D.##; for the Neuro Imaging for Coma Emergence and Recovery Consortium

### ABSTRACT

**Background:** Prognostication in comatose survivors of cardiac arrest is a major clinical challenge. The authors' objective was to determine whether an assessment with diffusion tensor imaging, a brain magnetic resonance imaging sequence, increases the accuracy of 1 yr functional outcome prediction in cardiac arrest survivors.

**Methods:** Prospective, observational study in two intensive care units. Fifty-seven comatose survivors of cardiac arrest

\* Assistant Professor, §§ Professor, Service de Réanimation, † Assistant Professor, Service de Neuroradiologie, \*\* Resident, School of Medicine, ## Professor, Service d'Anesthésie-Réanimation, Groupe Hospitalier Pitié-Salpêtrière, Assistance Publique-Hôpitaux de Paris, Université Paris – Pierre-et-Marie-Curie, Paris, France. ‡ Engineer, || Associate Professor, Division of Neuroscience Critical Care, Johns Hopkins University School of Medicine, Baltimore, Maryland. § Professor, Neurology Department and Cyclotron Research Centre University and University Hospital of Liège Sart Tilman, Liège, Belgium. ||| Professor, Unité INSERM UMR 5678, Université Paris – Pierre-et-Marie-Curie, Paris, France. # Professor, Department of Radiology, Massachusetts General Hospital, Harvard Medical School, Boston, Massachusetts. †† Professor, Service de Neuroradiologie, Hôpital Michalon, Grenoble, France. ‡‡ Professor, Service d'Anesthésie-Réanimation, Hôpital Central, Nancy, France.

Received from Université Paris, Pierre-et-Marie-Curie, Service de Réanimation, Service de Neuroradiologie, Anesthésie and Intensive Care Department, Groupe Hospitalier Pitié-Salpêtrière, Paris, France; INSERM UMR\_5678; Neurology Department and Cyclotron Research Centre, Liège, Belgium; Division of Neuroscience, Johns Hopkins University School of Medicine, Baltimore, Maryland; Service de Neuroradiologie, Hôpital Michalon, Grenoble, France; and Service d'Anesthésie-Réanimation, Hôpital Central, Nancy, France. Submitted for publication April 16, 2012. Accepted for publication August 31, 2012. Funded by a grant from the French Ministry of Health, Paris, France (Programme Hospitalier de Recherche Clinique 2005 #051061) and from the "Agence Nationale de la Recherche" for the program "investissements d'avenir" under Agreement n° ANR-10-IAIHU-06 to the Paris Institute of Translational Neurosciences-IHU-A-ICM. This work was presented at the 24th annual congress of the European Society of Intensive Care Medicine, Berlin, Germany, October 1–5 2011. Trial Registration clinicaltrials.gov Identifier: NCT00577954.

Address correspondence to Dr. Luyt: Service de Réanimation Médicale, Institut de Cardiologie, Groupe Hospitalier Pitié-Salpêtrière, 47, boulevard de l'Hôpital, 75651 Paris Cedex 13, France. charles-edouard.luyt@pssl.aphp.fr. Information on purchasing reprints may be found at [www.anesthesiology.org](http://www.anesthesiology.org) or on the masthead page at the beginning of this issue. ANESTHESIOLOGY's articles are made freely accessible to all readers, for personal use only, 6 months from the cover date of the issue.

Copyright © 2012, the American Society of Anesthesiologists, Inc. Lippincott Williams & Wilkins. Anesthesiology 2012; 117:00-00

### What We Already Know about This Topic

- Cardiac arrest is a leading cause of severe brain damage and carries a high risk of death or long-term disability
- Outcome prediction based on clinical examination or electrophysiologic evaluation is poor, especially when therapeutic hypothermia is used

### What This Article Tells Us That Is New

- One-year functional outcome in comatose survivors of cardiac arrest was predicted with a 94% sensitivity and 100% specificity using a magnetic resonance imaging index of white matter damage
- Magnetic resonance imaging evaluation of white matter injury may improve outcome prediction in patients 7–15 days after cardiac arrest

underwent brain magnetic resonance imaging. Fractional anisotropy (FA), a diffusion tensor imaging value, was measured in predefined white matter regions, and apparent diffusion coefficient was assessed in predefined grey matter regions. Prediction of unfavorable outcome at 1 yr was compared using four prognostic models: FA global, FA selected, apparent diffusion coefficient, and clinical classifiers.

**Results:** Of the 57 patients included in the study, 49 had an unfavorable outcome at 12 months. Areas under the receiver operating characteristic curve (95% CI) to predict unfavorable outcome for the FA global, FA selected, clinical, and apparent diffusion coefficient models were 0.92 (0.82–0.98), 0.96 (0.87–0.99), 0.78 (0.65–0.88), and 0.86 (0.74–0.94), respectively. The FA selected model had the best overall accuracy for predicting outcome, with a score above 0.44 having 94% (95% CI, 83–99%) sensitivity and 100% (95% CI, 63–100%) specificity for the prediction of unfavorable outcome.

**Conclusion:** Quantitative diffusion tensor imaging indicates that white matter damage is widespread after cardiac arrest. A prognostic model based on FA values in selected white matter tracts seems to predict accurately 1 yr functional outcome. These preliminary results need to be confirmed in a larger population.

CARDIAC arrest is a leading cause of severe brain damage and carries a high risk of death or long-term disability,<sup>1–3</sup> underscoring the need for timely, accurate, and

reliable methods to predict outcomes.<sup>4,5</sup> Existing prognostic models are based on clinical examination (*e.g.*, absence of motor, pupillary, or corneal reflexes) or on electrophysiologic evaluation (*e.g.*, bilateral absence of somatosensory cortical evoked responses with median-nerve stimulation [N20]) recorded within the first week after cardiac arrest.<sup>1,3</sup> However, preservation of brainstem or electrophysiologic responses does not rule out unfavorable outcomes. The brainstem is less vulnerable to anoxic–ischemic damage than the cerebral cortex; hence, brainstem reflexes may persist alongside extensive cortical damage, leading to outcomes such as the vegetative state.<sup>6</sup> The presence of normal median-nerve stimulation signals fails to discriminate patients with favorable outcome from those who do poorly.<sup>7,8</sup> Serum biomarkers such as neuron-specific enolase and S100  $\beta$ -protein correlate with the extent of neurologic injury, but data are limited regarding their prognostic value in the clinical setting.<sup>9,10</sup> Moreover, an increasing proportion of patients with cardiac arrest are managed with therapeutic hypothermia, which is associated with a significant reduction in the accuracy of outcome prediction when clinical and electrophysiologic variables are used.<sup>11</sup>

Evidence suggests that the type, severity, and anatomical distribution of injury detected with magnetic resonance imaging (MRI) may yield valuable prognostic information in patients with cardiac arrest.<sup>2,12–15</sup> These studies relied on regional or global measurements of apparent diffusion coefficient (ADC), which is a scalar quantity closely related to the mean diffusivity of water molecules in a voxel; this scalar expresses the propensity of water diffusion in any direction within a voxel. Using quantitative vector indices derived from diffusion tensor imaging (DTI), it is possible to measure the directional preference of water molecules and hence to make inferences about the underlying tissue microarchitecture. Fractional anisotropy (FA) is an index derived from the three Eigenvalues that describes the degree of directionality of water in the tissue, and changes in FA indicate white matter disorganization.<sup>16–18</sup> Using ADC, it has been shown that extensive white matter damage occurs in the acute setting of cardiac arrest. We postulated that DTI would provide valuable insights on the nature of anoxic–ischemic brain damage. Specifically, we tested the hypothesis that the accuracy of long-term functional outcome prediction is increased by addition of quantitative FA compared with prediction based on clinical variables or on ADC.

## Materials and Methods

### Study Design and Oversight

This prospective, multicenter, observational study was approved by the institutional review board of Pitié–Salpêtrière Hospital (Paris, France) and Liège University (Liège, Belgium). Written informed consent was obtained from the control subjects directly; consent was obtained from all patients' next of kin at the time of inclusion. Written informed consent for data collection and for follow-up was obtained directly from patients who regained consciousness.

### Patients

Patients were enrolled between October 2006 and March 2010 in two intensive care units (ICU) in Paris (France) and Liège (Belgium). Patients were eligible after the first week after a cardiac arrest if they met the following criteria: (1) age between 18 and 75 yr (inclusive); and (2) persistent unresponsiveness defined as the inability to follow simple commands after sedation was discontinued. Patients were excluded if they: (1) had a neurologic disease before cardiac arrest (*e.g.*, stroke, neurodegenerative conditions, or brain tumor); (2) were deemed moribund (expected survival <24 h); and (3) had a contraindication to the MRI, or presented with physiologic instability precluding transport and MRI scanning (*e.g.*, increased intracranial pressure, hemodynamic instability, or respiratory failure).

After enrollment, patients underwent multimodal brain MRI. To obtain normative MRI data, we enrolled 70 healthy volunteers who all underwent the same MRI scanning sequence as the patients.

### MRI Scan and Analysis

During the MRI scan, all patients were accompanied by a physician and vital signs were continuously monitored (continuous electrocardiogram, pulse oximetry, and capnography), as required by the study protocol. All patients were mechanically ventilated during the MRI scan.

Magnetic resonance images were acquired on 1.5 T or 3 T magnetic resonance units from two different manufacturers (General Electric Healthcare, Velizy, France, and Siemens Medical Solutions, Brussels, Belgium). Quadratic or multi-channel head coils were used. The precise parameters of each sequence (*e.g.*, echo time [TE] and repetition time [TR]) were adapted to the individual specifications of each manufacturer and the scanner. The following sequences were acquired:

1. A sagittal T1-weighted (1.5 T) or T2-weighted (3 T) sequence, used as a localizer for all remaining sequences.
2. A T2/fluid attenuated inversion recovery–weighted acquisition, using the bicallosal plane, with a 5-mm thickness, no gap, 240 mm field of view (FOV), and 256 × 256 matrix.
3. A T2\*–weighted acquisition, using the bicallosal plane, with a 5-mm thickness, no gap, 240 mm FOV, and 256 × 256 matrix.
4. A T2-weighted acquisition covering the brainstem and the basal ganglia, performed along the axial plane perpendicular to the main B0 field, with a 3-mm thickness, no gap, 240 mm FOV, and 256 × 256 matrix.
5. A 3D inversion recovery T1-weighted sequence (3D multiplanar reconstruction/3D fast spoiled gradient-echo) 240 mm FOV, and 1 mm isotropic voxel.
6. A diffusion tensor acquisition acquired in an axial plane perpendicular to the main field B0. The following parameters were used: gradient (B) applied in at least 11 directions (range 11–64), with a value of 1,000 mT/m; a

series without the diffusion gradient (the low-B image); FOV of 300 mm; matrix size 96 × 96; parameters for the DTI acquisitions were as follows according to the time period during which the patient was included:

7. center 1 (Paris—General Electric Healthcare)
  - 1.5 T (12 directions): 3-mm thickness, no gap, 11 directions, matrix 96 × 96, FOV = 28 cm, TR = 10,000, TE = 87
  - 1.5 T (23 directions): 5-mm thickness, no gap, 23 directions, matrix 96 × 96, FOV = 28 cm, TR = 8,000, TE = 80
  - 3 T (12 directions): 3-mm thickness, no gap, 12 directions, matrix 96 × 96, FOV = 28 cm, TR = 12,000, TE = 81.9
  - 3 T (50 directions): 2.5 mm thickness, no gap, 50 directions, matrix 128 × 128, FOV = 28 cm, TR = 14,000, TE = 84.5
8. center 2 (Liège—Siemens)
  - 3 T (20 directions): 3-mm thickness, no gap, 20 directions, matrix 96 × 96, FOV = 28 cm, TR = 5,700, TE = 87
  - 3 T (64 directions): 3-mm thickness, no gap, 64 directions, matrix 96 × 96, FOV = 28 cm, TR = 5,700, TE = 87

Time of acquisition for fluid attenuation inversion recovery was 3 min and 40 s, and for DTI = 8–10 min, depending on the sequence. At least seven controls were acquired per sequence.

The preprocessing of the diffusion tensor images was accomplished with FSL software<sup>\*\*\*</sup>. The diffusion tensor images were first corrected for distortions caused by eddy currents using the  $b = 0$  volume as reference. A diffusion tensor model was fitted for each voxel, and two diffusion parameters were extracted (FA and mean diffusivity) to build two parametric maps. Then, for each subject, the FA map was registered on a  $1 \times 1 \times 1 \text{ mm}^3$  standard space image (MNI152 space) using a nonlinear registration procedure (the so-called nonlinear registered maps). The same nonlinear transformation was then applied to the mean diffusivity map.<sup>19</sup> In addition to these nonlinear registrations, which did not take into account the residual misalignments between subjects, we used the tract-based spatial statistics approach to measure the DTI parameters within the FA skeleton.<sup>20</sup>

To characterize white matter integrity of each individual, we measured FA in the skeleton, a representation of the alignment-invariant tracts of the brain (fig. 1). The skeleton was segmented in 20 predefined white matter regions, which were selected from a white matter tracts atlas designed by Mori *S et al.*<sup>†††</sup> (fig. 2). To account for intercenter and intersequence variability, the FA values were normalized. The normalization

process consisted of scaling the FA of a patient by the mean of the FA calculated from the control group acquired in the same center and with the same imaging sequence.

ADC values were obtained using the mean diffusivity values in nine regions of interest of the grey matter (GM) as previously described.<sup>12,14,21</sup> The nine regions of interest were the following: caudate nucleus, putamen, thalamus, cerebellum, frontal lobe, insula, occipital lobe, parietal lobe, and temporal lobe.<sup>12,14,21</sup> Although hippocampus is particularly vulnerable in anoxia, it is a small region located close to the mastoid and thus subject to major artifacts on the DTI acquisition. It was not analyzable as a separate structure and was thus included in the temporal lobe region analysis. As for DTI parameters, to account for intercenter and intersequence variability, the ADC values were normalized. The normalization process consisted of scaling each value of a patient by the mean of the corresponding parameter calculated from the control group acquired in the same center and with the same imaging sequence.

The above processing, and all subsequent analysis of the MRI data, was performed by investigators who were blinded to the clinical information and outcomes data. The results of the MRI analysis were not provided to the clinical team caring for the patient in the ICU or the rehabilitation center.

### Patient Outcome Assessment

All patients were followed up until death or 12 months after cardiac arrest in survivors. Evaluation was performed by telephone or *via* an in-person visit. The principal outcome measure was the extended version of the Glasgow Outcome Scale (GOS-E), which was measured by blinded assessors.<sup>22,23</sup> This scale classifies patients into eight categories as follows: GOS-E score of 1, death; 2, vegetative state; 3, lower severe disability; 4, upper severe disability; 5, lower moderate disability; 6, upper moderate disability; 7, lower good recovery; and 8, upper good recovery. Any GOS-E score from 1 to 4 was defined as an “Unfavorable Outcome,” whereas a score from 5 to 8 was defined as a “Favorable Outcome.”

### Statistical Analysis

Normally distributed variables were expressed as mean ± SD and non-normally distributed variables as median [25th, 75th interquartile range]. Patients with favorable outcome (GOS-E ≥ 5) were compared with patients with unfavorable outcome (GOS-E < 5). Continuous variables were compared using the Student *t* test or the Mann–Whitney U test, as appropriate. Categorical variables were compared using the chi-squared test. FA variables were compared using repeated-measures analysis of variance with *post hoc* Fisher test.

To compare the predictive power of FA variables with clinical variables and ADC values in the GM, patients were grouped according to their outcome, favorable or unfavorable. Support vector machine classification was used for outcome prediction<sup>‡‡‡</sup>. For the classification model selection,

\*\*\* <http://www.fmrib.ox.ac.uk/fsl/>. Accessed August 22, 2012.

††† <http://www.csie.ntu.edu.tw/~cjlin/libsvm/>. Accessed August 22, 2012.

‡‡‡ [http://www.loni.ucla.edu/ICBM/Downloads/Downloads\\_DTI-81.shtml](http://www.loni.ucla.edu/ICBM/Downloads/Downloads_DTI-81.shtml). Accessed August 22, 2012.

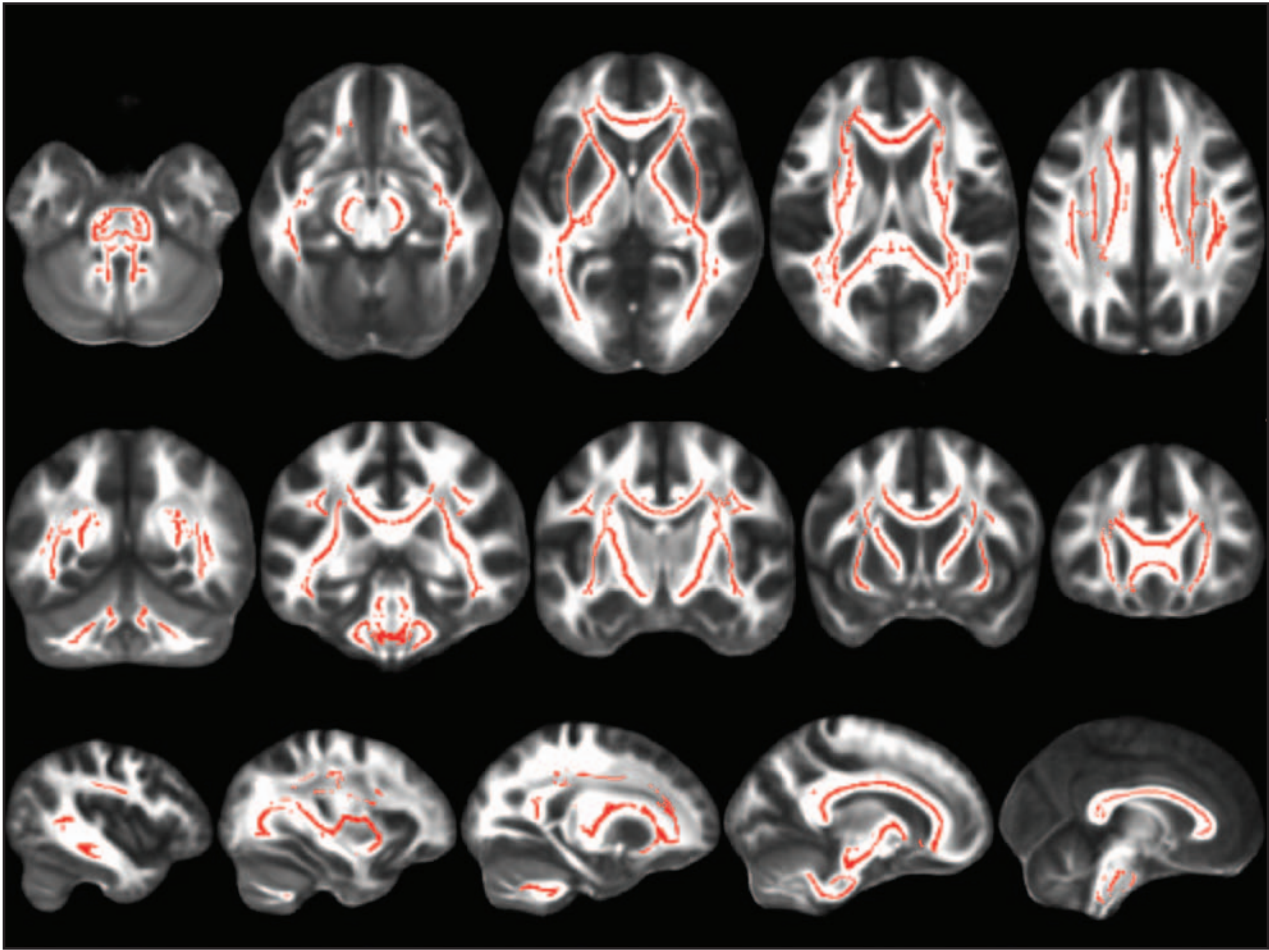


**Fig. 1.** Representation of the fractional anisotropy skeleton (in red), which is a representation of the alignment-invariant tracts of the brain.

we used the Radial basis function as kernel, and the best parameters of this function were found by a grid search using cross-validation (leave-one-out), maximizing the classification accuracy. In addition to the predicting class label, we also generated probabilistic scores by extending the support vector machine theory: the classification process also assigned to each patient an estimated probability that he or she belongs to the class of favorable or unfavorable outcome (the so-called classification score).

By using this methodology, we designed different classification models based on mean FA values within the 20 white matter regions of interest and based on the mean ADC values within the nine GM regions of interest. For classification models based on regional FA measurements (corresponding to 20 features), we tested two approaches: the first one consisted in building a model from all the 20 features (the so-called FA global model that generated FA global scores for each patient); the second one selected the best features among the 20 available to obtain the most discriminative model (the so-called FA selected model that generated FA selected scores for each patient). Then, we built a classification model based on ADC measurements within GM that

generated the so-called grey matter-ADC (GM-ADC) score for each patient.<sup>12,14,21</sup>

To compare the result of MRI scores (FA global, FA selected, and GM-ADC scores) with clinical data, a clinical prognostic model was constructed on the basis of the neurologic examination recorded on the day of the MRI. This clinical prognostic model was constructed using multivariable analysis that used all clinical data available on the day of MRI (the neurologic examination was performed by intensivists and included Glasgow Coma Scale, response to painful stimuli, and pupillary and corneal reflexes). The best clinical model to predict unfavorable outcome retained the following parameters: absence of pupillary reflexes, motor response to painful stimulus classified as bad (none, extension, or abnormal flexion), and absence of corneal reflexes. The weight of each parameter was adjusted based on the predicted probabilities in the logistic regression model. The four outcomes prediction models (clinical, FA global, FA selected, and GM-ADC scores) were compared by area under the receiver operating characteristic (ROC) curve analysis. We hypothesized that FA scores (global and selected scores) would predict unfavorable outcome with higher

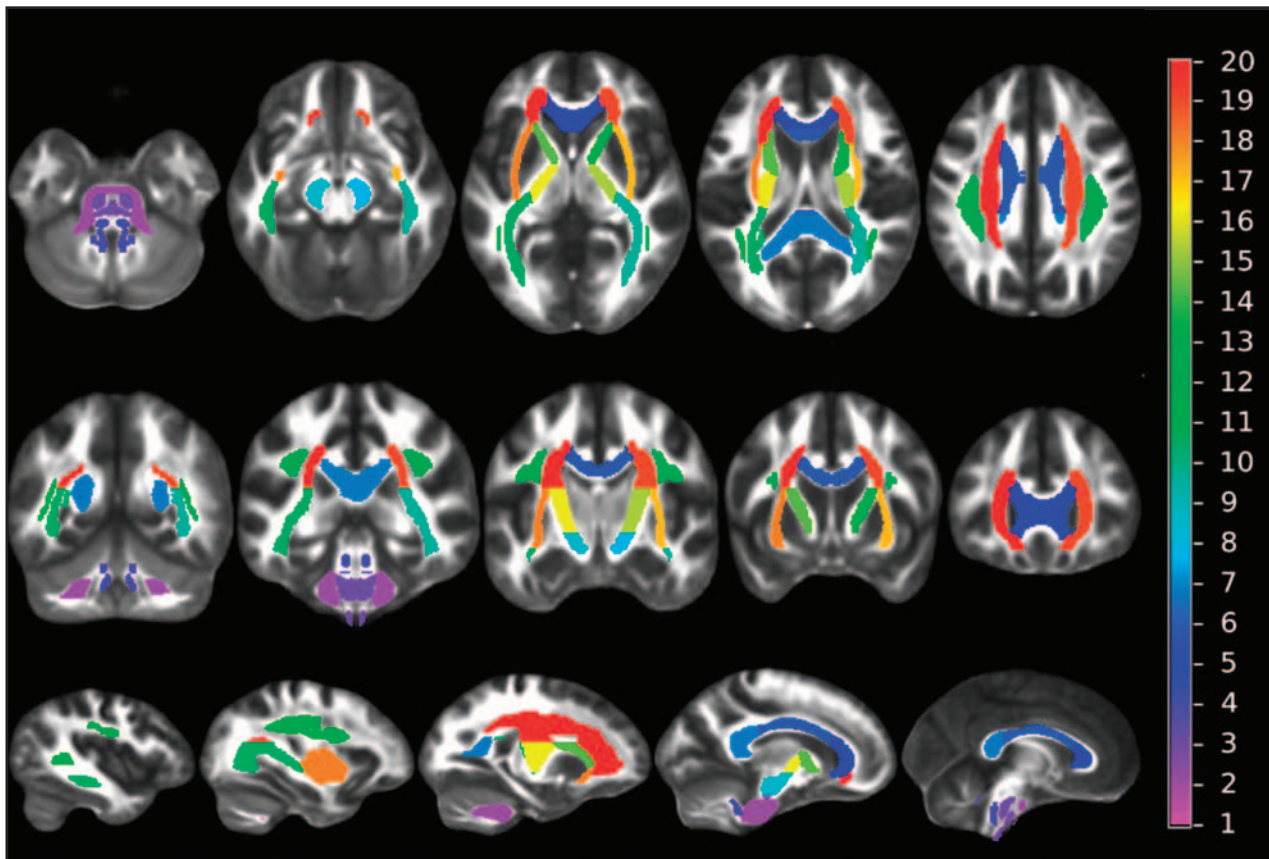


**Fig. 2.** Anatomical distribution of the 20 regions adapted from the study by Mori S *et al.* 1 = median cerebral peduncle; 2 = anterior brainstem; 3 = posterior brainstem; 4 = genu of the corpus callosum; 5 = body of the corpus callosum; 6 = splenium of the corpus callosum; 7 = right cerebral peduncle; 8 = left cerebral peduncle; 9 = right striatum; 10 = left striatum; 11 = right superior longitudinal fascicle; 12 = left superior longitudinal fascicle; 13 = right anterior limb of the internal capsule; 14 = left anterior limb of the internal capsule; 15 = right limb of the internal capsule; 16 = left limb of the internal capsule; 17 = right external capsule; 18 = left external capsule; 19 = right corona radiata; 20 = left corona radiata.

specificity than GM-ADC and clinical scores. Moreover, we hypothesized that FA scores would have greater areas under ROC than GM-ADC and clinical scores. All *P* values were two-tailed, and statistical significance was defined as a *P* value of less than 0.05. Analyses were performed using StatView 5.0 (SAS Institute Inc., Cary, NC) and SPSS 11.5 (SPSS Inc., Chicago, IL) software.

## Results

During the study period, 244 patients were admitted to the participating ICUs after cardiac arrest, of whom 63 (26%) were enrolled in the study and underwent MRI scanning. The principal reasons for nonenrollment were early death from multiorgan failure or brain death and emergence from coma (fig. 3). Six of the 63 enrolled patients were excluded from analysis because their MRI data were not interpretable (because of movement's artifacts in two cases and technical problems in four cases). Among the 57 remaining patients, 49 (86%) had an unfavorable outcome and 8 (14%) had a favorable outcome (fig. 1). Forty-two of the 49 patients with unfavorable outcome died (35 in the ICU). All deaths

(ICU or after hospital discharge) were directly or indirectly secondary to neurologic injury. Median [interquartile range] delay from cardiac arrest to death in these 42 patients was 17 [11–73] days. Among the seven with poor neurologic outcome who survived, GOS-E of 2, 3, and 4 was seen in four, one, and two patients, respectively. Among the eight patients with good outcome, three had a GOS-E of 5, one a GOS-E of 7, and four a GOS-E of 8. Admission characteristics of the patients according to their outcome are presented in table 1; there were no significant differences between patients with favorable and unfavorable outcome. The control subjects had no history of neurologic disease; 52% were male and their mean age was  $34 \pm 12$  yr.

Median [interquartile range] times from cardiac arrest to outcome evaluation were 12 [12–14] months for the nine patients with good outcome and 12 [8–12] months for the seven survivors with poor outcome. Neurologic examination of patients on the day of the MRI scan is given in table 2; Glasgow Coma Scale and its motor response component were significantly worse in patients with poor outcome. All patients were comatose at the time of MRI except

two patients whose Glasgow Coma Scale was 13 (MRI was ordered when they were still comatose and not cancelled).

The FA values in the 20 regions of interest are presented in figure 4. Although FA values were not different between patients with favorable outcome and controls, they were significantly lower in all regions of interest in patients with unfavorable outcome compared with patients with favorable outcome ( $P < 0.0001$ ) and compared with controls ( $P < 0.0001$ ).

The model based on selected features selected three features among the 20 corresponding to the mean FA within the following regions of interest: the anterior limb of the left internal capsule, the genu of the corpus callosum, and the body of the corpus callosum. This model (FA selected score) was found to be the most accurate for predicting unfavorable outcome. The area under the ROC curve of the FA selected algorithm was compared with that of the algorithms for FA global, clinical, and GM-ADC scores (fig. 5). For these four prediction algorithms, the areas under the ROC curves and their respective 95% CI were: 0.96 (0.87–0.99); 0.92 (0.82–0.98); 0.78 (0.65–0.88); and 0.86 (0.74–0.94). Comparisons of ROC curves showed that the FA selected score had a trend toward higher area under the curve compared with the GM-ADC score ( $P = 0.09$ ) and the clinical model ( $P = 0.07$ ) (fig. 5). To predict unfavorable outcome, a clinical score cutoff value of 0.96 had a sensitivity of 90% (95% CI, 78–97%) and a specificity of 63% (95% CI, 25–91%); a GM-ADC score cutoff value of 0.91 had a sensitivity of 83% (95% CI, 70–93%) and a specificity of 88% (95% CI, 47–98%); an FA global score cutoff value of 0.77 had a sensitivity of 80% (95% CI, 66–90%) and a specificity of 100% (95% CI, 63–100%); and an FA selected score cutoff value of 0.44 had a sensitivity of 94% (95% CI, 83–99%) and a specificity of 100% (95% CI, 63–100%).

To eliminate any possibility that morphologic MRI (mainly, fluid attenuated inversion recovery and diffusion) might have influenced the decision-making process during the course of the ICU stay, we performed a second analysis on the 22 ICU survivors (15 with poor outcome and the seven with good outcome). Their characteristics and clinical data at the time of inclusion were similar to that of the overall population and of the ICU nonsurvivors, whereas neurologic examination on the day MRI was performed was worse in ICU nonsurvivors than in ICU survivors (see table 3). In this analysis, similar results were observed: the areas under the ROC curves and their respective 95% CI of the FA selected score, FA global score, clinical score, and GM-ADC score were 1 (0.84–1), 0.93 (0.83–0.99), 0.67 (0.44–0.85), and 0.83 (0.61–0.95), respectively. Comparisons of ROC curves showed that area under the curve of FA selected score was higher than that of the GM-ADC score ( $P = 0.05$ ) and the clinical model ( $P < 0.001$ ). To predict unfavorable outcome in those ICU survivors, a clinical score cutoff value of 0.96 had a sensitivity of 71% (95% CI, 42–91%) and a specificity of 63% (95% CI, 25–91%); a GM-ADC score cutoff value of 0.91 had a sensitivity of 79% (95% CI, 49–95%) and a specificity of 88% (95% CI, 47–98%); an FA global score cutoff value of 0.77 had a sensitivity of 79% (95% CI, 49–95%) and a specificity of 100% (95% CI, 63–100%); and an FA selected score cutoff value of 0.44 had a sensitivity of 100% (95% CI, 77–100%) and a specificity of 100% (95% CI, 63–100%).

In a further analysis that included only the 36 patients treated with hypothermia, the same results were observed: the area under the ROC curve was higher with the FA selected score compared with the clinical model and the GM-ADC score. The same results were observed in another

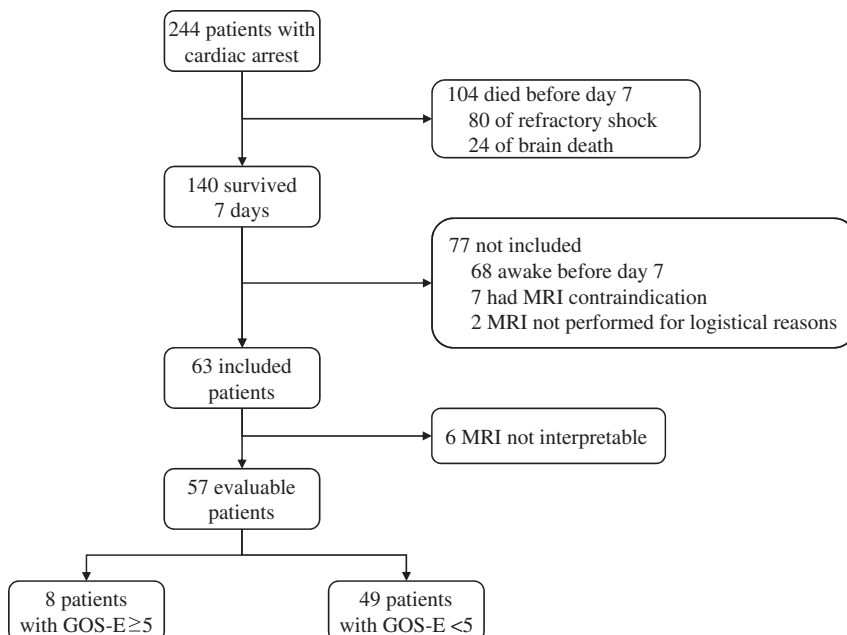


**Fig. 3.** Flowchart of the study. GOS-E = Glasgow Outcome Scale extended; MRI = magnetic resonance imaging.

**Table 1.** Patients Characteristics

Variables	Overall Population	Good Outcome	Poor Outcome
	N = 57	n = 8	n = 49
Age, yr	52 ± 18	46 ± 17	53 ± 18
Male sex, n (%)	40 (70)	7 (88)	32 (65)
McCabe & Jackson score for comorbidity ≥ 2	6 (11)	0	6 (13)
Place of CA			
Out-of-hospital	49 (86)	8 (100)	45 (85)
In-hospital	8 (14)	0	8 (15)
Cause of cardiac arrest			
Primary cardiac cause	47 (82)	8 (100)	39 (80)
Other	10 (18)	0	10 (20)
No-flow time (min. without CPR)	5 [0–10]	10 [5–10]	5 [0–10]
Low-flow time (min. with CPR)	20 [10–36]	25 [15–39.5]	20 [10–36]
Hypothermia induction	36 (63)	7 (88)	29 (59)
GCS at admission	3	3	3
Admission biological variables			
Troponin, ng/ml *	1.1 [0.1–7.7]	7.9 [1.2–48.3]	0.48 [0.1–4.4]
Lactate, mM	5.1 [2.3–9.1]	5.7 [2.4–9.6]	5.0 [2.3–8.9]
Type of MRI			
1.5 T	26 (46)	3 (38)	23 (47)
3 T	31 (54)	5 (63)	26 (53)

Results are expressed as mean ± SD, median [25, 75 interquartile] or n (%).

\* Data obtained for 40 patients in the poor outcome group and in all patients in the good outcome group.  $P < 0.05$  for between-groups comparison.

CA = cardiac arrest; CPR = cardiopulmonary resuscitation; GCS = Glasgow Coma Scale; MRI = magnetic resonance imaging; T = Tesla.

**Table 2.** Clinical Evaluation at the Time of Magnetic Resonance Imaging

	Overall Population	Good Outcome	Poor Outcome
	N = 57	N = 8	N = 49
Time from CA to MRI, d	11 [7–17]	10 [8–14]	11 [7–17]
GCS *	5 [3–7]	8 [7–13]	5 [3–7]
Absence of pupillary reflexes	4 (7)	0	4 (8)
Absence of corneal reflexes	2 (4)	0	2 (4)
Motor response *†			
Good	10 (18)	3 (37)	5 (10)
Bad	47 (82)	5 (63)	44 (90)

Results are expressed as median [25, 75 interquartile] or n (%).

\*  $P < 0.05$ . † Response to painful stimulus classified as bad (none, extension, or abnormal flexion) or good (localizes painful stimuli or obeys command).

CA = cardiac arrest; GCS = Glasgow Coma Scale; MRI = magnetic resonance imaging.

analysis that included only the 49 out-of-hospital patients with cardiac arrest.

## Discussion

Early identification of outcomes after cardiac arrest is important because it may inform decisions regarding therapeutic intensity and goals of care. Current prognostic tools based on clinical or electrophysiologic variables either lack specificity or are useful only in identifying patients with the most severe

brain damage.<sup>1</sup> To our knowledge, this is the first large-scale, bicenter study evaluating DTI in comatose survivors after cardiac arrest. It shows that the FA score is highly predictive of the long-term clinical outcome: a FA selected score more than 0.44 had a sensitivity of 94% (95% CI, 83–99%) and a specificity of 100% (95% CI, 63–100%) for predicting unfavorable outcome. In other words, all patients with an FA selected score more than 0.44 had a poor outcome, that is, death or severe neurologic disability (GOS-E < 5). The

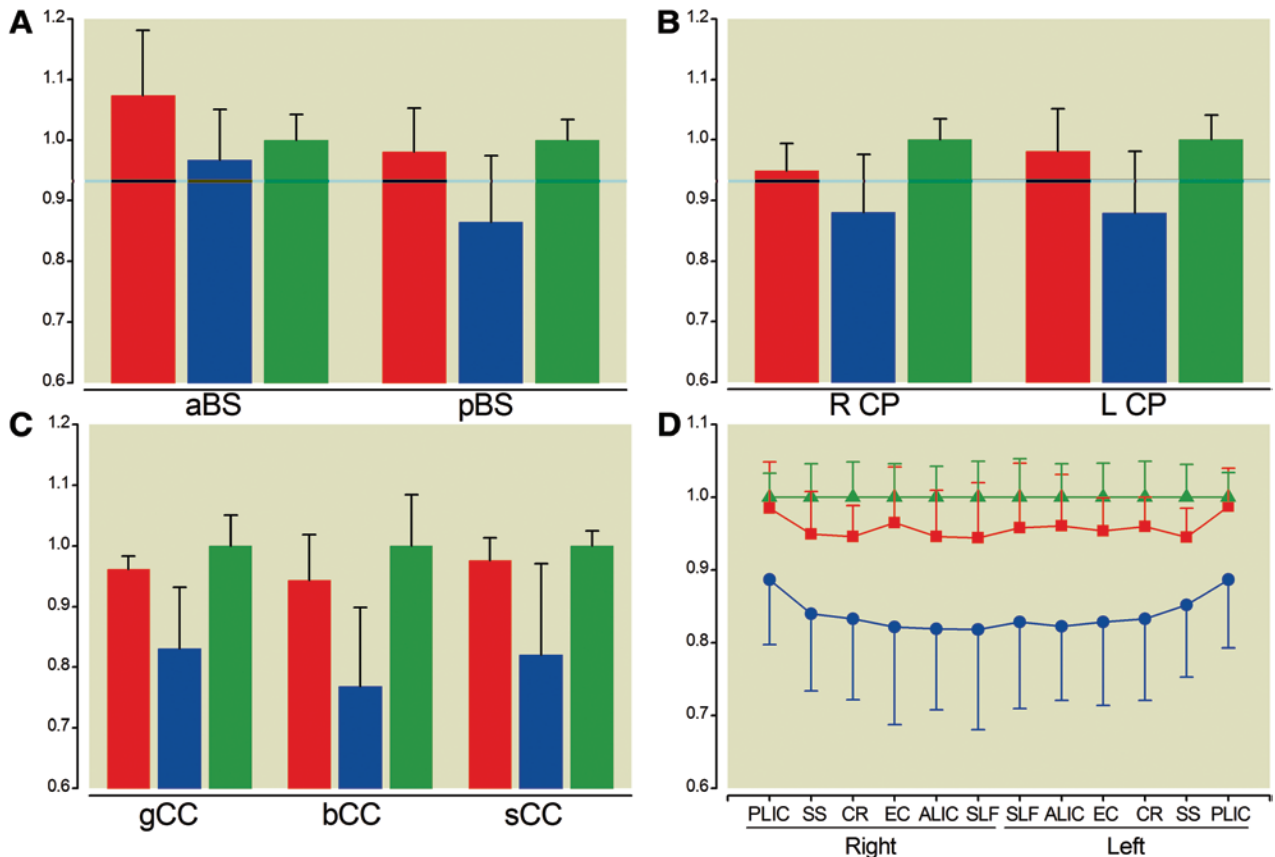


**Fig. 4.** Fractional anisotropy values in the 20 regions of the white matter in patients with favorable outcome (red bars and diamonds), unfavorable outcome (blue bars and squares) and in controls (green bars and triangles). Values are expressed as means  $\pm$  SD. A, Values in aBS and pBS. B, Values in R CP and L CP. C, Values in the gCC, sCC, and bCC. D, Values in the right and left PLIC, SS, CR, EC, ALIC, and SLF.  $P < 0.001$  for comparisons between patients with unfavorable outcome and controls or patients with favorable outcome. aBS = anterior brainstem; pBS = posterior brainstem; L CP = left cerebral peduncles; R CP = right cerebral peduncles; gCC = genu corpus callosum; sCC = splenium corpus callosum; bCC = body corpus callosum; PLIC = posterior limb of the internal capsules; SS = striatum; CR = corona radiate; EC = external capsules; ALIC = anterior limbs of the internal capsules; SLF = superior longitudinal fascicles.

FA scores (FA selected score or FA global score) had trend toward greater prognostic accuracy than scores based on clinical variables and the previously published MRI variables obtained in the GM (*i.e.*, ADC values)<sup>12,14,21</sup>: although the clinical model or the GM-ADC score-based model had high specificity in patient classification, the rate of false-negative prediction remained high.

Several recent studies evaluated diffusion-weighted MRI as a prognostic tool in cardiac arrest.<sup>2,12–14,24</sup> All found that ADC was lower in deceased or poor-outcome patients, sometimes with conflicting results. Wu *et al.*<sup>12</sup> found that whole brain median ADC less than  $665 \times 10^{-6} \text{ mm}^2/\text{s}$  was a significant predictor of poor outcome (based on no eyes opening or a 6-month Rankin scale  $> 3$ ); on the other hand, Wijman *et al.*<sup>24</sup> found that mean ADC value over the entire brain did not differentiate between patients with favorable outcome and those with unfavorable outcome.<sup>12,24</sup> However, this study did establish that the percentage of brain volume with an ADC value below a threshold of  $650\text{--}700 \times 10^{-6} \text{ mm}^2/\text{s}$  best differentiated between survivors and nonsurvivors;

similarly, the percent volume of brain below an ADC threshold of  $400\text{--}450 \times 10^{-6} \text{ mm}^2/\text{s}$  was able to differentiate unfavorable from favorable outcome among the survivors.<sup>24</sup> The latter study seems to suggest that size and spatial distribution of the injury is more important than the raw decrease in the overall mean ADC value of the brain. More recently, in a series of 39 survivors of cardiac arrest, Choi *et al.*<sup>15</sup> have shown that the presence of diffusion-weighted imaging hyperintense lesions in both the cortex and basal ganglia are strongly associated with a poor outcome. These authors also identified the ADC thresholds for outcome prediction with 100% specificity.<sup>15</sup> In our study, the ADC of the GM had good sensitivity and specificity to predict unfavorable outcome, but its accuracy was lower than that in DTI.

Most studies evaluating cardiac arrest survivors with diffusion-weighted imaging were single center and involved a relatively small sample size. Moreover, because of the rapid time-dependent variation of ADC, MRI was performed early (2–5 days) after the cardiac arrest. Transportation out of the ICU at this stage, when many patients with cardiac arrest

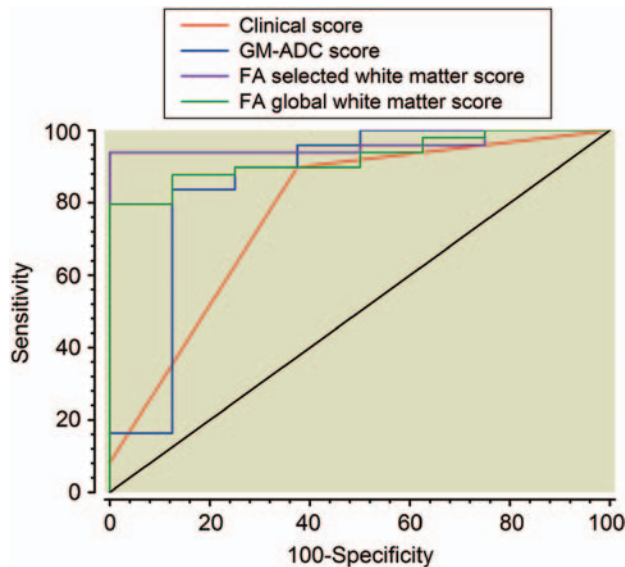


**Fig. 5.** Receiver operating characteristic curves of the clinical score, the GM-ADC score, the FA global score, and the FA selected score to predict unfavorable outcome. Areas under the ROC curves and their respective 95% CI were 0.78 (0.65–0.88), 0.86 (0.74–0.94), 0.92 (0.82–0.98), and 0.96 (0.87–0.99).  $P = 0.07$  for comparison between FA selected and GM-ADC scores.  $P = 0.09$  for comparison between FA selected and clinical scores.  $P > 0.1$  for other comparisons. FA = fractional anisotropy; GM-ADC = grey matter apparent diffusion coefficient.

remain hemodynamically unstable, is potentially associated with significant risks.<sup>25</sup> We were able to overcome some of these limitations because our study was performed in two centers and because MRIs were acquired at a later stage (7–15 days) after hemodynamic and respiratory stabilization.

Another major limitation of prognostic studies in patients with anoxic–ischemic encephalopathy is that the clinicians are not fully blinded to the result of the tests (and in particular, the MRI studies). Therefore, some clinical decisions could have potentially been based on the results of the test used for prognostication. This may lead to the so-called “self-fulfilling prophecies.”<sup>25</sup> In our study, DTI data were analyzed at the end of the study by an investigator blinded to the clinical status of the patients, and clinicians were not aware of the results, although they had access to the morphologic images (fluid attenuated inversion recovery and diffusion). To overcome these limitations, we restricted the analysis to the subgroup of patients who survived after the ICU stay, and our results remained similar: the DTI score was superior to GM-ADC and clinical scores for predicting outcome. The analysis of this subset of patients allows us to observe effects that would be independent of early non-neurologic deaths that might have altered the results. Indeed, some patients with neurologic recovery might have died early because of sepsis, multiorgan failure, or other complications in the ICU.

DTI can characterize the architecture of the white matter by exploring the diffusion of water molecules in the brain.<sup>18</sup> Among the parameters obtained from the three

Eigenvalues of the diffusion tensor, FA describes the degree of directionality of water in the tissue, and its modifications represent the white matter disorganization.<sup>18,26</sup> This variable provides greater anatomical and functional information than the scalar parameters such as ADC.<sup>17,27,28</sup> We hypothesized that its value in anoxic patients could be of interest.<sup>29</sup> Our results confirmed this hypothesis, because the FA algorithms were more accurate than clinical or ADC algorithms. Our data are concordant with previously published data in infants suffering from hypoxic–ischemic encephalopathy.<sup>29,30</sup> In these patients, FA has been found to be reduced in the white matter, and FA had a superior predictive power for tissue injury than ADC.<sup>29,30</sup> Moreover, it has been shown that DTI correlated with histologic data; in a 58-yr-old man who remained comatose after cardiac arrest, had an MRI with DTI acquisition, and subsequently died from sepsis, the authors found that histology of the brain was in accordance with DTI data, demonstrating extensive demyelination and widespread axonal loss.<sup>18</sup>

Our data suggest that in the early phase of anoxic–ischemic encephalopathy after cardiac arrest, damage is seen in white matter and GM. This is consistent with knowledge of the vascular anatomy of the deep cerebral white matter that contains widespread linear arterioles with few anastomoses. This anatomy adds to the vulnerability of the central white matter to hypoxic–ischemic injury.<sup>31–33</sup>

Some limitations of our study should be recognized. First, only a limited number of patients had favorable outcome. This is due to the design of the study: indeed, only patients not responding to simple orders at least 7 days after cardiac arrest were included. This criterion was established to maximize the safety of MRI and to avoid transportation of patients that awakened rapidly after cardiac arrest and in whom the indication of MRI could be of debate. Because of the limited number of patients included and the low number of patients with favorable outcome (8 of 57), the accuracy of our models predicting unfavorable outcome could have been due to chance rather than to the precision of the model itself and thus to the accuracy of the MRI. Including a larger number of patients and validating these data in a validation cohort are the only ways to avoid this bias and confirm the validity of our results. Thus, our results need to be prospectively validated in a larger cohort, which can be obtained only in a large multicenter study. Another potential limitation is the fact that the prognostication algorithm did not take into account clinical data at the time of the cardiac arrest and during the course of the hospital stay. For example, the first noted cardiac rhythm, presence of bystander and bystander basic life support, use of therapeutic hypothermia, and the results of coronary angiogram were not incorporated in the outcome prediction. It is therefore implicitly assumed that either these variables have no effect on the outcome or that their effect is reflected in the DTI parameters. This hypothesis is partially supported by the superiority of the FA score over the algorithm based on the clinical parameters.

**Table 3.** Patients' Characteristics as a Function of ICU Survival

Variables	Overall Population	ICU Survivors	ICU Nonsurvivors
	N = 57	n = 22	n = 35
Age, yr	52 ± 18	48 ± 19	55 ± 17
Male sex, n (%)	40 (70)	17 (77)	23 (66)
McCabe & Jackson score for comorbidity ≥ 2	6 (11)	5 (23)	1 (3)
Place of CA			
Out-of-hospital	49 (86)	19 (86)	30 (86)
In-hospital	8 (14)	3 (14)	5 (14)
Cause of cardiac arrest			
Primary cardiac cause	47 (82)	16 (73)	31 (89)
Other	10 (18)	6 (27)	4 (11)
No-flow time (min. without CPR)	5 [0, 10]	5 [0, 10]	5 [0, 10]
Low-flow time (min. with CPR)	20 [10, 36]	20 [9, 30]	25 [14, 40]
Hypothermia induction	36 (63)	14 (64)	22 (63)
GCS at admission	3	3	3
Admission biological variables			
Troponin, ng/ml *	1.1 [0.1, 7.7]	1.6 [0.4, 7.9]	0.7 [0.1, 7.3]
Lactate, mM	5.1 [2.3, 9.1]	5.8 [4.7, 10.8]	3.3 [1.9, 7.1]
Type of MRI			
1.5 T	26 (46)	11 (50)	15 (43)
3 T	31 (54)	11 (50)	20 (57)
Time from CA to MRI, d †	11 [7, 17]	15 [8, 21]	8 [7, 13]
Neurologic examination before MRI			
GCS †	5 [3, 7]	7 [5, 8]	5 [3, 6]
Absence of pupillary reflexes	4 (7)	0	4
Absence of corneal reflexes	2 (4)	0	2
Motor response ††			
Good	10 (18)	9 (41)	1 (3)
Bad	47 (82)	13 (59)	34 (97)

\* Data obtained for 16 patients in the ICU survivors group and for 32 patients in the ICU nonsurvivors group. †  $P < 0.05$  between ICU survivors and nonsurvivors. ‡ Response to painful stimulus classified as bad (none, extension, or abnormal flexion) or good (localizes painful stimuli or obeys command).

CA = cardiac arrest; CPR = cardiopulmonary resuscitation; GCS = Glasgow Coma Scale; ICU = intensive care unit; MRI = magnetic resonance imaging; T = Tesla.

However, the clinical outcome prediction model we used was limited to a few neurologic signs and may have failed to capture the wealth of predictive information that is available clinically. Third, we used variables from the day of MRI in our clinical model rather than standardizing these variables to a fixed date, for example at day 3 after cardiac arrest. However, because of aggressive resuscitation in such patients (and the use of hypothermia), clinical data may not be pertinent at day 3 because some patients receive sedation or are still in shock, conditions that alter neurologic examination. Fourth, we did not perform a standardized neurologic examination in the first week after hospital admission in all patients, in particular for patients who had early recovery of consciousness. However, this limitation does not alter our results; indeed, the purpose of this preliminary study was to evaluate the value of DTI in patients who remained comatose 1 week after cardiac arrest. Finally, the control groups we used for

regional FA (mean diffusivity) data normalization were only sequence- and region-matched but not age-matched.

In conclusion, brain MRI using DTI reveals extensive white matter damage in patients with anoxic–ischemic brain injury after cardiac arrest. DTI seems to be a promising tool to predict unfavorable outcome in comatose survivors of cardiac arrest; however, these results need to be confirmed in a larger population. Whether DTI could be useful or not to predict outcome in all patients early after cardiac arrest remained to be determined.

## References

1. Wijdicks EF, Hijdra A, Young GB, Bassetti CL, Wiebe S; Quality Standards Subcommittee of the American Academy of Neurology: Practice parameter: Prediction of outcome in comatose survivors after cardiopulmonary resuscitation (an evidence-based review): Report of the Quality Standards Subcommittee of the American Academy of Neurology. *Neurology* 2006; 67:203–10

2. Topcuoglu MA, Oguz KK, Buyukserbetci G, Bulut E: Prognostic value of magnetic resonance imaging in post-resuscitation encephalopathy. *Intern Med* 2009; 48:1635–45
3. Young GB: Clinical practice. Neurologic prognosis after cardiac arrest. *N Engl J Med* 2009; 361:605–11
4. Mancini ME, Soar J, Bhanji F, Billi JE, Dennett J, Finn J, Ma MH, Perkins GD, Rodgers DL, Hazinski MF, Jacobs I, Morley PT; Education, Implementation, and Teams Chapter Collaborators: Part 12: Education, implementation, and teams: 2010 International Consensus on Cardiopulmonary Resuscitation and Emergency Cardiovascular Care Science With Treatment Recommendations. *Circulation* 2010; 122(16 Suppl 2):S539–81
5. Hazinski MF, Nolan JP, Billi JE, Böttiger BW, Bossaert L, de Caen AR, Deakin CD, Drajer S, Eigel B, Hickey RW, Jacobs I, Kleinman ME, Kloeck W, Koster RW, Lim SH, Mancini ME, Montgomery WH, Morley PT, Morrison LJ, Nadkarni VM, O'Connor RE, Okada K, Perlman JM, Sayre MR, Shuster M, Soar J, Sunde K, Travers AH, Wyllie J, Zideman D: Part 1: Executive summary: 2010 International Consensus on Cardiopulmonary Resuscitation and Emergency Cardiovascular Care Science With Treatment Recommendations. *Circulation* 2010; 122(16 Suppl 2):S250–75
6. Fried TR, Bradley EH, Towle VR, Allore H: Understanding the treatment preferences of seriously ill patients. *N Engl J Med* 2002; 346:1061–6
7. Zandbergen EG, de Haan RJ, Stoutenbeek CP, Koelman JH, Hijdra A: Systematic review of early prediction of poor outcome in anoxic-ischaemic coma. *Lancet* 1998; 352:1808–12
8. Robinson LR, Micklesen PJ, Tirschwell DL, Lew HL: Predictive value of somatosensory evoked potentials for awakening from coma. *Crit Care Med* 2003; 31:960–7
9. Shinozaki K, Oda S, Sadahiro T, Nakamura M, Hirayama Y, Abe R, Tateishi Y, Hattori N, Shimada T, Hirasawa H: S-100B and neuron-specific enolase as predictors of neurological outcome in patients after cardiac arrest and return of spontaneous circulation: A systematic review. *Crit Care* 2009; 13:R121
10. Wojtczak-Soska K, Lelonek M: S-100B protein: An early prognostic marker after cardiac arrest. *Cardiol J* 2010; 17:532–6
11. Rossetti AO, Oddo M, Logroscino G, Kaplan PW: Prognostication after cardiac arrest and hypothermia: A prospective study. *Ann Neurol* 2010; 67:301–7
12. Wu O, Sorensen AG, Benner T, Singhal AB, Furie KL, Greer DM: Comatose patients with cardiac arrest: Predicting clinical outcome with diffusion-weighted MR imaging. *Radiology* 2009; 252:173–81
13. Järnum H, Knutsson L, Rundgren M, Siemund R, Englund E, Friberg H, Larsson EM: Diffusion and perfusion MRI of the brain in comatose patients treated with mild hypothermia after cardiac arrest: A prospective observational study. *Resuscitation* 2009; 80:425–30
14. Mlynash M, Campbell DM, Leproust EM, Fischbein NJ, Bammer R, Eyngorn I, Hsia AW, Moseley M, Wijman CA: Temporal and spatial profile of brain diffusion-weighted MRI after cardiac arrest. *Stroke* 2010; 41:1665–72
15. Choi SP, Park KN, Park HK, Kim JY, Youn CS, Ahn KJ, Yim HW: Diffusion-weighted magnetic resonance imaging for predicting the clinical outcome of comatose survivors after cardiac arrest: A cohort study. *Crit Care* 2010; 14:R17
16. Basser PJ, Jones DK: Diffusion-tensor MRI: Theory, experimental design and data analysis - a technical review. *NMR Biomed* 2002; 15:456–67
17. Beaulieu C: The basis of anisotropic water diffusion in the nervous system - a technical review. *NMR Biomed* 2002; 15:435–55
18. Kremer S, Renard F, Noblet V, Mialin R, Wolfram-Gabel R, Delon-Martin C, Achard S, Schenck M, Mohr M, Dietemann JL, Schneider F: Diffusion tensor imaging in human global cerebral anoxia: Correlation with histology in a case with autopsy. *J Neuroradiol* 2010; 37:301–3
19. Basser PJ, Pierpaoli C: Microstructural and physiological features of tissues elucidated by quantitative-diffusion-tensor MRI. *J Magn Reson B* 1996; 111:209–19
20. Smith SM, Jenkinson M, Johansen-Berg H, Rueckert D, Nichols TE, Mackay CE, Watkins KE, Ciccarelli O, Cader MZ, Matthews PM, Behrens TE: Tract-based spatial statistics: Voxelwise analysis of multi-subject diffusion data. *Neuroimage* 2006; 31:1487–505
21. Mazziotta J, Toga A, Evans A, Fox P, Lancaster J, Zilles K, Woods R, Paus T, Simpson G, Pike B, Holmes C, Collins L, Thompson P, MacDonald D, Iacoboni M, Schormann T, Amunts K, Palomero-Gallagher N, Geyer S, Parsons L, Narr K, Kabani N, Le Goualher G, Boomsma D, Cannon T, Kawashima R, Mazoyer B: A probabilistic atlas and reference system for the human brain: International Consortium for Brain Mapping (ICBM). *Philos Trans R Soc Lond, B, Biol Sci* 2001; 356:1293–322
22. Teasdale G, Jennett B: Assessment of coma and impaired consciousness. A practical scale. *Lancet* 1974; 2:81–4
23. Hudak AM, Caesar RR, Frol AB, Krueger K, Harper CR, Temkin NR, Dikmen SS, Carlile M, Madden C, Diaz-Arrastia R: Functional outcome scales in traumatic brain injury: A comparison of the Glasgow Outcome Scale (Extended) and the Functional Status Examination. *J Neurotrauma* 2005; 22:1319–26
24. Wijman CA, Mlynash M, Caulfield AF, Hsia AW, Eyngorn I, Bammer R, Fischbein N, Albers GW, Moseley M: Prognostic value of brain diffusion-weighted imaging after cardiac arrest. *Ann Neurol* 2009; 65:394–402
25. Galanaud D, Puybasset L: Cardiac arrest - has the time of MRI come? *Crit Care* 2010; 14:135
26. Kumar R, Woo MA, Macey PM, Fonarow GC, Hamilton MA, Harper RM: Brain axonal and myelin evaluation in heart failure. *J Neurol Sci* 2011; 307:106–13
27. Song SK, Sun SW, Ramsbottom MJ, Chang C, Russell J, Cross AH: Demyelination revealed through MRI as increased radial (but unchanged axial) diffusion of water. *Neuroimage* 2002; 17:1429–36
28. Song SK, Yoshino J, Le TQ, Lin SJ, Sun SW, Cross AH, Armstrong RC: Demyelination increases radial diffusivity in corpus callosum of mouse brain. *Neuroimage* 2005; 26:132–40
29. van Pul C, Buijs J, Janssen MJ, Roos GF, Vlaardingerbroek MT, Wijn PF: Selecting the best index for following the temporal evolution of apparent diffusion coefficient and diffusion anisotropy after hypoxic-ischemic white matter injury in neonates. *AJNR Am J Neuroradiol* 2005; 26:469–81
30. Ward P, Counsell S, Allsop J, Cowan F, Shen Y, Edwards D, Rutherford M: Reduced fractional anisotropy on diffusion tensor magnetic resonance imaging after hypoxic-ischemic encephalopathy. *Pediatrics* 2006; 117:e619–30
31. Ginsberg MD, Myers RE: The topography of impaired microvascular perfusion in the primate brain following total circulatory arrest. *Neurology* 1972; 22:998–1011
32. Ginsberg MD, Hedley-Whyte ET, Richardson EP Jr: Hypoxic-ischemic leukoencephalopathy in man. *Arch Neurol* 1976; 33:5–14
33. Busl KM, Greer DM: Hypoxic-ischemic brain injury: Pathophysiology, neuropathology and mechanisms. *NeuroRehabilitation* 2010; 26:5–13